



Letter

The ANC of ^{16}O states from $^7\text{Be} + ^{12}\text{C}$ α -transfer reaction to study $^{12}\text{C}(\alpha,\gamma)^{16}\text{O}$

K. Kundalia ^{a,1}, D. Gupta ^{a,*}, Sk M. Ali ^{a,2}, R. Mitra ^a, Swapan K. Saha ^{a,3},
O. Tengblad ^b, A. Perea ^b, I. Martel ^c, J. Cederkall ^d, A.M. Moro ^e

^a Department of Physical Sciences, Bose Institute, EN 80 Sector V, Bidhannagar, Kolkata, 700091, India

^b Instituto de Estructura de la Materia-CSIC, Serrano 113 bis, ES-28006, Madrid, Spain

^c University of Huelva, Av. Fuerzas Armadas s/n. Campus "El Carmen", Huelva, 21007, Spain

^d Department of Physics, Lund University, Box 118, SE-221 00, Lund, Sweden

^e Departamento de Física Atómica, Molecular y Nuclear, Facultad de Física, Universidad de Sevilla, Apartado 1065, E-41080, Sevilla, Spain



ARTICLE INFO

Editor: Prof. Betram Blank

PACS:

25.55.Hp

25.60.-t

26.20.Fj

Keywords:

Stellar helium burning

Transfer reactions

ANC

ABSTRACT

We measured the angular distributions for the $^{12}\text{C}(^7\text{Be},^3\text{He})^{16}\text{O}$ transfer reaction at 35 MeV leading to several excited states of ^{16}O . The angular distribution of the ground state of ^{16}O was measured for the first time in this reaction. The corresponding Asymptotic Normalization Coefficients (ANC) of all the observed states were determined. The ANC of ground state, 6.92 MeV (2^+) and 7.12 MeV (1^-) subthreshold states of ^{16}O obtained from this work are utilized to determine the astrophysical $E1$ and $E2$ S -factors of the $^{12}\text{C}(\alpha,\gamma)^{16}\text{O}$ reaction in an R -matrix analysis.

1. Introduction

In nuclear astrophysics, the α -capture reaction $^{12}\text{C}(\alpha,\gamma)^{16}\text{O}$ is being studied for decades as a key reaction in the helium-burning phase of stars [1]. This reaction along with the preceding triple- α fusion reaction forming ^{12}C determines the C/O abundance ratio in stars. This ratio is crucial for stellar nucleosynthesis of elements heavier than carbon [2, 3]. The final fate of a star is determined by this ratio after the helium-burning cycle. The evolution of life in the universe depends on this ratio as well [4–6]. Thus, the reaction is said to be the “holy grail of nuclear astrophysics” [6]. However, the ^{12}C production rate is known within 15% uncertainty [7], while there is about 40% uncertainty [8] in the $^{12}\text{C}(\alpha,\gamma)^{16}\text{O}$ rate despite extensive studies. Thus, we are far away from the better than 10% uncertainty required by stellar models [4,9].

The direct capture cross section of the $^{12}\text{C}(\alpha,\gamma)^{16}\text{O}$ reaction at the Gamow energy of 300 keV is extremely small ($\sim 10^{-17}$ b), which precludes any direct measurement. Direct measurements down to $E_{\text{cm}} = 0.9$ MeV exist [10], but extrapolation to 300 keV remains difficult. This is due to the presence of the 6.92(2^+) and 7.12(1^-) MeV states of ^{16}O .

The partial waves $l = 1$ and 2 contribute, and it is challenging to extract the $E1$ and $E2$ contributions from $^{12}\text{C}(\alpha,\gamma)^{16}\text{O}$ cross section measurements. The α -spectroscopic factors (S_α) of the above two excited states spread over a large range of values [11] and during extrapolation, non-resonant capture and all possible contributions of the excited states need to be considered [7]. It may be noted that, angular distribution of the above reaction was also obtained recently by measuring the inverse reaction with gamma beams [12].

In this scenario, the efficient indirect technique of studying α -cluster transfer reactions to populate the relevant states in the residual nuclei is very useful. Such studies provide information that complement those from (α,γ) capture and (α,α) scattering measurements. The loosely bound stable isotopes ^6Li and ^7Li with prominent α -cluster structures, have been widely used in studies of $^6,7\text{Li} + ^{12}\text{C}$ populating ^{16}O states [7,13,14]. The transfer reaction $^{12}\text{C}(^11\text{B},^7\text{Li})^{16}\text{O}$ has also been studied [15] in this context. However, the breakup contributions in these reactions affected the transfer channel to a great extent.

Earlier, the angular distribution of $^{12}\text{C}(^7\text{Li},t)$ reaction at 34 MeV was studied by Becchetti et al. [16], in a finite-range DWBA framework. The

* Corresponding author.

E-mail addresses: kundalia.kabita@eli-np.ro (K. Kundalia), dhruba@jcbosc.ac.in (D. Gupta).

¹ Present address: Extreme Light Infrastructure - Nuclear Physics, IFIN-HH, 077125, Magurele, Romania.

² Present address: FRIB, Michigan State University, East Lansing, MI 48824, USA.

³ Visiting faculty, School of Astrophysics, Presidency University, 86/1 College Street, Kolkata 700073, India.

obtained S_α value for the 6.92 MeV state was smaller than the theoretical value, while it was opposite for the 7.12 MeV state. They also studied the $^{12}\text{C}(^6\text{Li},d)^{16}\text{O}$ reaction at 42 MeV [17], and predicted a larger stellar helium burning rate in the older stars greater than one-solar mass, from the obtained S_α value. The calculations of Keeley [18] compared the elastic scattering angular distributions for ^7Be and ^7Li on a ^{208}Pb target at around 30–40 MeV. A pronounced Coulomb rainbow was absent for ^7Be and it was concluded that breakup affects ^7Be more strongly than ^7Li , primarily due to its lower breakup threshold.

Now, the ^7Be nucleus has a prominent α -cluster structure, and a low breakup threshold of 1.58 MeV. Rudchik et al., [19] studied the properties of ^7Li and ^7Be at similar energies on a lighter mass target ^9Be . The study shows that the difference in the breakup threshold of ^7Li and ^7Be has no effect in nuclear dominated scattering, as opposed to the Coulomb-dominated scattering studied by Keeley [18]. Sgourous et al. [20] studied the $^7\text{Be} + ^{28}\text{Si}$ reaction at 13–22 MeV and compared it with similar data for $^6,^7\text{Li}$. Low statistics and geometrical efficiency of their detector setup hindered the identification of any ^3He - ^4He coincidence events. However, CDCC calculations estimated the breakup contribution to be small. Measurements of $^7\text{Be} + ^{58}\text{Ni}$ reaction was carried out by Mazzocco et al. at 21.5 MeV [21]. No detection of coincident ^3He - ^4He indicated low breakup cross section (σ_{bu}) that is consistent with CDCC calculations. The experimental yields of ^3He (^4He) were found to contribute 31% (24%) from breakup and an estimate of $\sigma_{bu} \sim 10.8$ mb was obtained.

The work of Amro et al. [22] on $^7\text{Be} + ^{12}\text{C}$ at nearly the same energy as ours, recorded very few coincidences between ^3He and ^4He . The observed yield of ^3He is small as compared to ^4He . They report that the $^{12}\text{C}(^7\text{Be},^3\text{He})^{16}\text{O}$ reaction rates from their experiment are larger than extant data on Li-induced α -transfer reactions at similar beam energies [16,23,24]. Both Refs. [21,22] report that there is indication of direct α -transfer as the main mechanism contributing to the observed ^3He yield [25]. It will be more apparent later in this work, that there exists a substantial discrepancy in the ANC values of ^{16}O from various works involving transfer and breakup reactions and R-matrix analysis.

The low breakup yield makes ^7Be an excellent candidate for the study of high excitation α -cluster states in the residual nuclei. However, in the work of Amro et al. [22], the uncertainty in the optical model parameters (OMP) owing to limited angular distributions posed a serious problem in the study of the transfer reactions. One of the largest source of uncertainty to determine the ANC, is the uncertainty in the finite-range DWBA calculations. Improved measurements of the transfer reactions are thus required to constraint the values from the calculations. The present work reports the measurement of α -transfer reaction with $^7\text{Be} + ^{12}\text{C}$ at 35 MeV. The required OMP are obtained from elastic scattering data of the same experiment as reported in Ref [26].

Now, in the radiative capture reaction $^{12}\text{C}(\alpha,\gamma)^{16}\text{O}$, the α -capture proceeds predominantly through the 6.92 (2^+) and 7.12 (1^-) MeV excited states of ^{16}O [27]. To investigate the contribution of these two subthreshold resonances to the (α,γ) cross section, an evaluation of the α -reduced widths is required. In the present Letter, these states are populated through the α -cluster transfer reaction $^{12}\text{C}(^7\text{Be},^3\text{He})^{16}\text{O}^*$. In particular, the ground state (g.s.) is populated for the first time. The ANC of the states obtained from this work are utilized to determine the astrophysical $E1$ and $E2$ S -factors of the $^{12}\text{C}(\alpha,\gamma)^{16}\text{O}$ reaction in an R-matrix analysis. The impact of the g.s. ANC on the S -factors is also studied.

The organization of the paper is as follows. In Section 2, the experimental setup is briefly described. In Section 3 the transfer reaction data and analysis are reported. In Section 4, conclusions and outlook of the present work are discussed.

2. Experiment

The experiment was carried out at HIE-ISOLDE, CERN with a 35 MeV $^7\text{Be}^{4+}$ beam. The beam resolution was ~ 168 keV and the average beam intensity was $\sim 5 \times 10^5$ pps. A CD_2 target of thickness 15 μm was used

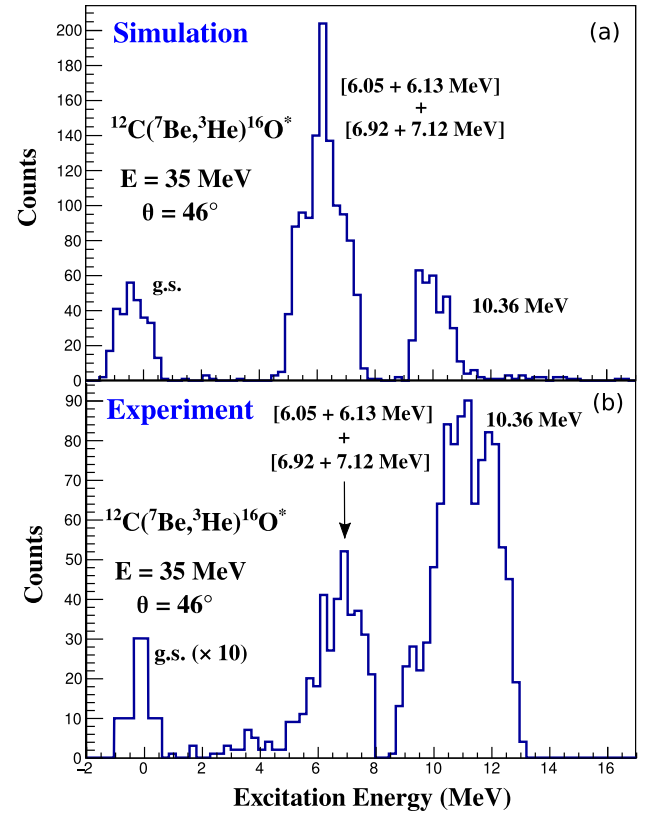


Fig. 1. Excitation energy spectrum of ^{16}O from $^7\text{Be} + ^{12}\text{C}$ α -transfer reaction at 35 MeV. The (a) NPTool simulations and (b) experimental data correspond to 46° at one of the telescopes of the pentagon detectors.

in the experiment. A 15 μm CH_2 and a 1 mg/cm^2 ^{208}Pb target were also used for background measurements and normalization purposes respectively. There were five $\Delta E - E$ telescopes consisting of 60 μm thick Micron W1 double-sided silicon strip detectors (DSSDs) backed by unsegmented Micron MSX25 pads of thickness 1000 μm . They were arranged in a pentagon geometry, covering $40^\circ - 80^\circ$ in lab. The forward angles from $8^\circ - 25^\circ$ were covered by a Micron S3 annular detector, while the back angles $127^\circ - 165^\circ$ were covered by two Micron BB7 DSSDs, backed by MSX40 unsegmented silicon pad detectors. The detailed experimental setup, beam production and energy calibrations are described in Ref. [26]. The present data include errors of 10% each due to beam intensity and target thickness, in addition to the statistical uncertainty in the yields.

3. Analysis

The excitation energy spectrum of ^{16}O from $^7\text{Be} + ^{12}\text{C}$ α -transfer reaction at 35 MeV is shown in Fig. 1. The simulations and the experimental data correspond to $\theta = 46^\circ$ at the pentagon detectors. The ground state is observed and the counts are multiplied by 10 in the figure for clarity. The breakup threshold of the ^{16}O nucleus into $\alpha + ^{12}\text{C}$ is 7.16 MeV [28]. There are two doublets [6.05 (0^+) + 6.13 (3^-)] MeV and [6.92 (2^+) + 7.12 (1^-)] MeV as subthreshold states. We could observe the contribution of these states as well as the 10.36 (4^+) MeV state, as shown in Fig. 1. There are several other neighbouring states near this state. However, the unnatural parity state 11.08 MeV (3^+) cannot be populated by a direct α -transfer. Also, the 11.097 MeV (4^+) state has a small α -decay width and is thereby not expected to be significantly populated by direct α -transfer [29].

The subthreshold doublets could not be resolved in the present work, as the energy resolution is ~ 660 keV [26]. The individual cross

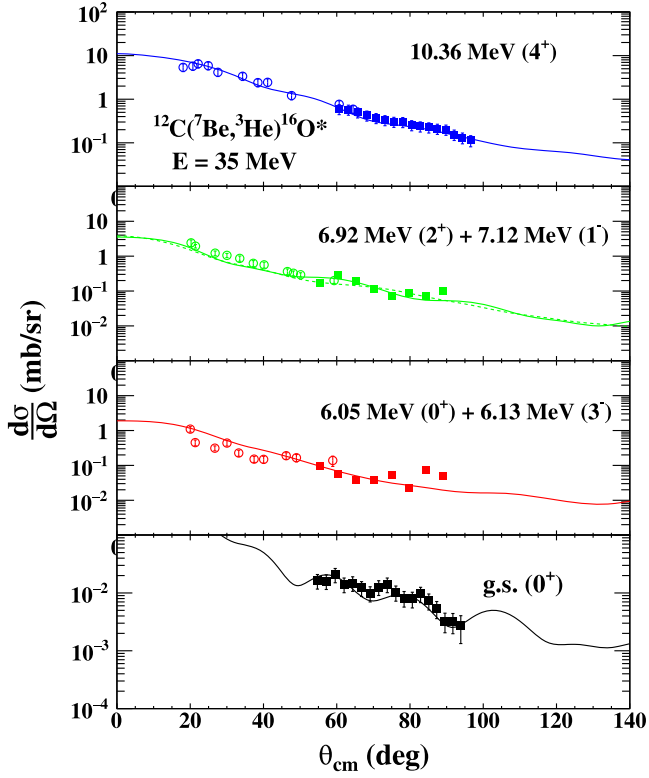


Fig. 2. Angular distributions for α -transfer reaction $^{12}\text{C}(^7\text{Be},^3\text{He})^{16}\text{O}^*$ at $E = 35$ MeV. Data for the g.s. and several excited states of ^{16}O are shown. The data in solid squares are from the present work, while the open circles are the data of Amro et al. [22] shown for comparison. The lines represent the DWBA calculations.

sections for the doublets are obtained by fitting the measured yields with two Gaussians, at energies corresponding to the known excitation energies of ^{16}O . The cross sections are normalized by using the elastic data from the same experiment [26]. The resulting angular distributions corresponding to the $J^\pi = 2^+/1^-$ and $0^+/3^-$ states are shown in Fig. 2. The angular distribution of the ground state of ^{16}O has been measured for the first time. The data of Amro et al. [22] are also shown in the figure for comparison. It is seen from Figs. 1, 2, that the ^{16}O states in the $^{12}\text{C}(^7\text{Be},^3\text{He})^{16}\text{O}^*$ reaction are populated and the angular distributions are forward peaked. The DWBA calculations on the present data, shown in Fig. 2 are carried out with the code FRESKO [30]. The required $^7\text{Be} + ^{12}\text{C}$ entrance channel potential parameters are taken from Ref. [26]. For the $^3\text{He} + ^{16}\text{O}$ exit channel, we started with the potentials from Zurmühle [31]. We fitted the data with SFRESKO [30], and obtained an improved set of potential parameters. The core-core potential for $^3\text{He} + ^{12}\text{C}$ is adopted from the global potential listed in the work of Perey and Perey [32]. The above potentials are listed in Table 1. The binding potentials for $\alpha + ^3\text{He}$ and $\alpha + ^{12}\text{C}$ are obtained from the works of Buck [33] and Bertulani [34] respectively. These are of Gaussian forms

Table 1

Optical model potential parameters for $^7\text{Be} + ^{12}\text{C}$ reaction at 35 MeV, $R_x = r_x \left(A_p^{\frac{1}{3}} + A_T^{\frac{1}{3}} \right)$.

System	V (MeV)	r_p (fm)	a_p (fm)	W (MeV)	r_w (fm)	a_w (fm)	r_c (fm)	Ref.
$^7\text{Be} + ^{12}\text{C}$	142.96	0.702	0.617	9.954	1.041	1.079	1.25	[26]
$^3\text{He} + ^{16}\text{O}$	78.81	0.992	0.592	15.24	0.929	1.033	0.763	[31]
$^3\text{He} + ^{12}\text{C}$	155.0	0.570	0.840	5.73	1.410	0.410	0.858	[32]

Table 2

The excitation energy (E_x), α -spectroscopic factors (S_α), single particle ANC ($b_{N,L}$), ANC ($C_{N,L}$) and ANC error ($\Delta C_{N,L}$) of ^{16}O states. The J^π values and the quantum numbers representing number of nodes and orbital angular momentum (N, L) are also given for each state.

E_x (MeV)	(N, L)	S_α	$b_{N,L}$ (fm $^{-\frac{1}{2}}$)	$C_{N,L}$ (fm $^{-\frac{1}{2}}$)	$\Delta C_{N,L}$ (fm $^{-\frac{1}{2}}$)
0.0 (0^+)	(2,0)	1.12	7.03×10^2	7.44×10^2	$\pm 1.34 \times 10^2$ (18%)
6.05 (0^+)	(4,0)	0.44	2.47×10^3	1.64×10^3	$\pm 0.71 \times 10^3$ (43%)
6.13 (3^-)	(1,3)	0.71	2.14×10^2	1.81×10^2	$\pm 0.31 \times 10^2$ (17%)
6.92 (2^+)	(3,2)	0.75	1.80×10^5	1.56×10^5	$\pm 0.27 \times 10^5$ (17%)
6.92 (2^+)	(2,2)	0.79	1.36×10^5	1.21×10^5	$\pm 0.21 \times 10^5$ (18%)
7.12 (1^-)	(2,1)	0.41	4.24×10^{14}	2.72×10^{14}	$\pm 1.60 \times 10^{14}$ (59%)

with depth of 83.77 and 85.9 MeV and radius of 2.52 and 2.80 fm respectively.

The α -spectroscopic factors for states of ^{16}O can be extracted from the ratio of the experimental transfer reaction cross sections to the theoretical calculations. Thus,

$$\frac{d\sigma}{d\Omega_{\text{exp}}} = S'_\alpha S_\alpha \frac{d\sigma}{d\Omega_{\text{DWBA}}} \quad (1)$$

where the spectroscopic factors S'_α and S_α correspond to the configurations of $\alpha + ^3\text{He}$ for the ground state of ^7Be and $\alpha + ^{12}\text{C}$ for the states of ^{16}O respectively. To obtain S'_α , we considered the microscopic overlap function for the $^7\text{Be} = \alpha + ^3\text{He}$ decomposition, evaluated with the no-core shell-model with continuum (NCSMC) calculations of Vorabbi et al. [35]. This was compared with the ^7Be ground-state wavefunction determined with the adopted $\alpha + ^3\text{He}$ potential. The value of S'_α was then determined to match the normalization of these two functions. The scaling factor is found to be 1.03 and thus the spectroscopic factor S'_α is 1.06. To determine S_α , it is considered as a free parameter in SFRESKO calculations for the ground state and 10.36 MeV state of ^{16}O . For the subthreshold states, since the experimental cross sections are obtained as the sum of two doublets (6.05 + 6.13) MeV and (6.92 + 7.12) MeV, the calculated cross sections of the two states in each doublet are added and the corresponding S_α varied simultaneously to obtain the best fit for the angular distribution.

Now, the ANC ($C_{N,L}$) of a particular state, is related to S_α by

$$C_{N,L}^2 = S_\alpha b_{N,L}^2 \quad (2)$$

where $b_{N,L}$ is the single particle ANC. It is apparent that $C_{N,L}$ is the amplitude of the overlap of the bound-state wave functions of the initial and final nuclei. Here, $b_{N,L}$ is the normalization of the bound state wave function of the residual nucleus (here ^{16}O) at large radii with respect to the Whittaker function [36]. It may be noted that $b_{N,L}$ also depends on the choice of potential parameters, like S_α . But the variations of these two quantities with the geometrical parameters of the bound state potential are opposite in nature. Thus, the ANC obtained from the product of these two quantities remains nearly constant with the change of potential parameters for a peripheral reaction. Table 2 gives the list of ANC obtained for the ground state and the subthreshold states. The bound state radial wave functions for the different states are calculated in FRESKO for a fixed set of the (N, L) quantum numbers. They represent, respectively, the number of nodes and the orbital angular momentum of the wave function for the transferred α -particle relative to the ^3He and ^{12}C cores. In FRESKO, N is associated with the number of nodes of the intercluster wavefunction, including the origin, but not the infinity, so $N > 0$. The corresponding values for all the states of ^{16}O are taken from the work of Belhout [11], where the (N, L) are determined in accordance with the "Wildermuth-Tang formula" [37]. An additional set of values $(N, L) = (3, 2)$ is considered for the 6.92 MeV state in the theoretical calculations, obtained using orthogonality condition model in the work of Suzuki et al. [38]. The resulting DWBA calculations are shown in Fig. 2 as solid and dotted lines for the (6.92 + 7.12) MeV doublet.

Table 3

Percentage error due to the chosen potential parameters in MeV and radius of the binding potential of ^{16}O in fm, contributing to the g.s. ANC of ^{16}O , in addition to the experimental error of 17%. See text for details.

Parameter	Value	Range	% Error
V_{entr}	142.96	137.0–147.0	5.05 %
W_{entr}	9.954	9.57–10.45	0.28 %
V_{exit}	78.81	77.93–79.60	0.70 %
W_{exit}	15.24	14.45–16.15	0.64 %
r_{BE}	2.80	2.18–2.96	3.24 %

To calculate the ANC error, we added the experimental errors in quadrature with the errors introduced due to the chosen potentials as explained below. The limits of the variation of the parameters are set according to the $\chi^2 + 1$ principle [39]. To start with, we have the entrance channel potential and the χ^2 value from fitting the elastic scattering data. The real potential depth is first changed until we get $\chi^2 + 1$. This yielded the minimum and maximum values of the potential depth. The same procedure is followed for all other parameters. Table 3 shows the range of the variation of the parameters and the resulting percentage error in the extraction of the ANC for the ground state. The depths of the real and imaginary potentials of the entrance (V_{entr} , W_{entr}) and exit (V_{exit} , W_{exit}) channels as well as the radius (r_{BE}) of the binding potential of ^{16}O were varied as explained earlier. In Table 2, the J^π values and the (N, L) quantum numbers of the transferred α -cluster are given for each state, in addition to the α -spectroscopic factors (S_α), single particle ANC ($b_{N,L}$), ANC ($C_{N,L}$) and ANC error ($\Delta C_{N,L}$) of the ^{16}O states. It can also be seen from Table 2 that the $\Delta C_{N,L}$ of 7.12 MeV state is substantially higher as compared to the 6.92 MeV state. The reason is the following. The theoretical cross sections for the 7.12 MeV state is about an order of magnitude smaller than that for the 6.92 MeV state. This resulted in a larger error for this state when fitting the data and obtaining the S_α for both states simultaneously. The same argument holds for the 6.05 MeV state as compared to the 6.13 MeV state of the other doublet.

In Fig. 3, the g.s. ANC values from earlier studies [40–44] are compared to the present work. The present value is consistent with those of Adhikari [40] within error bars, while it is about twice as large as the value from Shen [43]. Morais and Lichtenthaler [41] quoted three ANC values corresponding to their calculations using

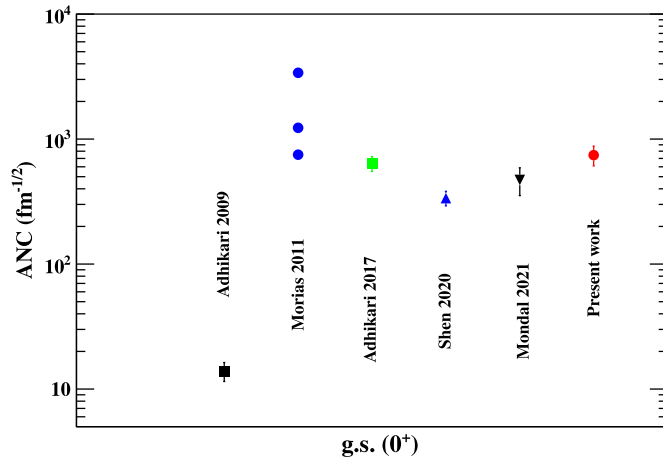


Fig. 3. The ANC for the ground state of ^{16}O from the breakup (^{16}O , α ^{12}C) [42] (black square) and α -transfer (^{16}O , ^{12}C) [41] (blue circle), ($^7\text{Li}, t$) [40] (green square), ($^{11}\text{B}, ^7\text{Li}$) [43] (blue upward triangle), (^{20}Ne , ^{16}O) [44] (black downward triangle), and the present work ($^7\text{Be}, ^3\text{He}$) (red circle). The three ANC values corresponding to Morais and Lichtenthaler [41] are due to calculations using three different sets of potentials. (For interpretation of the references to colour in this figure legend, the reader is referred to the web version of this article.)

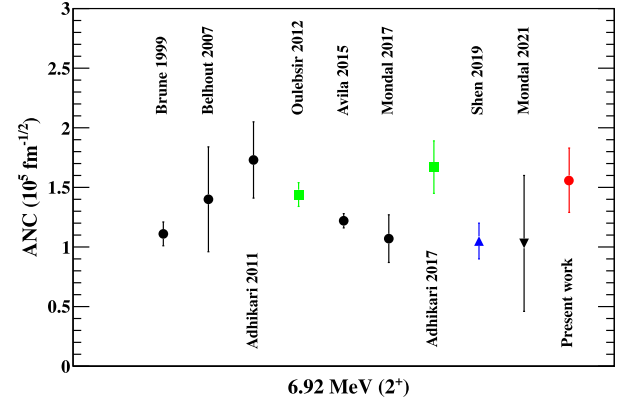


Fig. 4. The ANC for the 6.92 MeV (2^+) state of ^{16}O obtained from α -transfer reactions ($^6\text{Li}, d$) [11,45–48] (black circle), ($^7\text{Li}, t$) [7,40] (green square), ($^{11}\text{B}, ^7\text{Li}$) [15] (blue upward triangle), (^{20}Ne , ^{16}O) [44] (black downward triangle), and the present work ($^7\text{Be}, ^3\text{He}$) (red circle). (For interpretation of the references to colour in this figure legend, the reader is referred to the web version of this article.)

three different sets of potentials. The g.s. ANC and the 6.92 (2^+) subthreshold state ANC are highly correlated fit parameters in an R -matrix calculation [43]. This requires accurate determination of the gs ANC. The ground state γ decays, through the 6.92 and 7.12 MeV subthreshold states, have the most significant contributions to the total capture cross section [6,27]. In Fig. 4, the ANC value for the 6.92 MeV (2^+) state from the present work is compared to earlier data at sub-Coulomb energies by Brune [45] and above barrier energies by Oulebsir [7], Belhout [11], Shen [15], Adhikari [40,46], Avila [47], and Mondal [44,48]. The ANC value from the present work agrees with most of the earlier works within error bars and is an independent measurement by using ^7Be beam at a different energy.

To study the $^{12}\text{C}(\alpha, \gamma)^{16}\text{O}$ reaction rate, we carried out a multilevel phenomenological R -matrix calculation using the AZURE2 code [49,50] to estimate the g.s. $E1$ and $E2$ astrophysical S -factors for the $^{12}\text{C}(\alpha, \gamma)^{16}\text{O}$ reaction, using the ANC values from the present work. The calculations adopt a channel radius of 5.43 fm [6]. The $E1$ and $E2$ contributions were fitted independently on the extant capture data [51,52], and the best-fit parameters are obtained by χ^2 minimization. The bound and resonance parameters were kept fixed during fitting, while the background states were allowed to vary freely (Table 4). The ANC for the g.s., 6.92 and 7.12 MeV states were fixed at $744 \pm 134 \text{ fm}^{-1/2}$, $(1.56 \pm 0.27) \times 10^5 \text{ fm}^{-1/2}$, and $(2.72 \pm 1.6) \times 10^{14} \text{ fm}^{-1/2}$ respectively from the present work. For the $E2$ capture component, we included three states at 6.92, 9.85, and 11.52 MeV in addition to a higher-energy background-equivalent state to account for the contributions from the tails of other

Table 4

Bound and resonance parameters used in the R -matrix calculations of the astrophysical S -factors of the ground state $E1$ and $E2$ components. The values in the brackets are the fixed resonance parameters. J^π denotes the spin-parity of the ^{16}O state, E_x is the excitation energy, E_r is the resonance energy in the center-of-mass frame. The partial γ -decay widths (Γ_γ) and α -decay widths (Γ_α) for the 1^- and 2^+ states in ^{16}O are taken from Ref. [7].

J^π	E_x (MeV)	E_r (MeV)	C ($\text{fm}^{-1/2}$)/ Γ_α (keV)	Γ_γ (keV)
0^+	0.0	[−7.16]	$C = [744 \pm 134]$	
1^-	7.12	[−0.04]	$C = [(2.72 \pm 1.6) \times 10^{14}]$	$[5.5 \times 10^{-5}]$
1^-	9.58	[2.42]	$\Gamma_\alpha = [388.0]$	$[1.56 \times 10^{-3}]$
1^-	Background	12.8	$\Gamma_\alpha = 1054.6$	2.65×10^{-3}
2^+	6.92	[−0.24]	$C = [(1.56 \pm 0.27) \times 10^5]$	$[9.7 \times 10^{-5}]$
2^+	9.85	[2.68]	$\Gamma_\alpha = [0.76]$	$[5.7 \times 10^{-6}]$
2^+	11.52	[4.34]	$\Gamma_\alpha = [83.0]$	$[6.1 \times 10^{-4}]$
2^+	Background	7.8	$\Gamma_\alpha = 1250.8$	6.33×10^{-5}

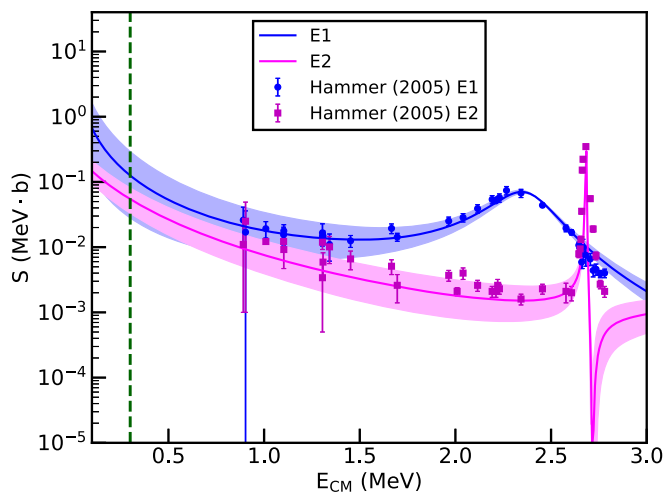


Fig. 5. R -matrix calculations for the g.s. $E1$ and $E2$ S -factors of the $^{12}\text{C}(\alpha,\gamma)^{16}\text{O}$ reaction obtained using the ANC values from the present work. The shaded blue and magenta bands represent the uncertainties in the S -factors arising from the uncertainties in the present ANC values. Experimental data points are taken from Refs. [51,52]. The green dashed line corresponds to the Gamow energy at 300 keV. (For interpretation of the references to colour in this figure legend, the reader is referred to the web version of this article.)

higher-lying 2^+ states. Similarly, the $E1$ capture component was modelled using two states at 7.12 and 9.58 MeV in addition to a background-equivalent state representing the tails of other higher-lying 1^- states.

The astrophysical S -factors for the g.s. $E1$ and $E2$ transitions are shown in Fig. 5 with the blue and magenta bands respectively. The uncertainties in the S -factors are due to the errors in the present ANC values. From the present R -matrix calculations, we obtain $S_{E1}(300 \text{ keV}) = 124.94^{+166.30}_{-97.1} \text{ keV b}$ and $S_{E2}(300 \text{ keV}) = 54.09^{+26.39}_{-21.22} \text{ keV b}$. The large uncertainty in the present $E1$ S -factor primarily arises from the 59% uncertainty in the present ANC value of the 7.12 MeV state. The central value of the present $E1$ S -factor at 300 keV is about 25% higher compared to those obtained using ($^6\text{Li,d}$) and ($^7\text{Li,t}$) reactions [7,45] due to the higher ANC value of the 7.12 MeV state from this work. The central value of the present $E2$ S -factor at 300 keV is in good agreement with the ($^7\text{Li,t}$) measurement [7]. We also investigated the impact of our higher g.s. ANC of $744 \text{ fm}^{-1/2}$ on the S_{E1} and S_{E2} components of the present R -matrix analysis, in comparison to the ANC value of $58 \text{ fm}^{-1/2}$ of Deboer [6]. It shows that a higher value of the g.s. ANC of ^{16}O has a negligible effect on $S_{E1}(300 \text{ keV})$. In contrast, the higher value of the g.s. ANC results in a decrease of $S_{E2}(300 \text{ keV})$ by approximately 40%.

4. Conclusion

In summary, we have measured the angular distributions for the transfer reaction $^{12}\text{C}(^7\text{Be},^3\text{He})^{16}\text{O}^*$ at $E = 35 \text{ MeV}$. The ground state of ^{16}O has been measured for the first time in this reaction. We utilized the optical potentials obtained from the same experiment [26], and this significantly improved on the earlier study by Amro et al. [22]. We report the S_α and ANC for the ground state and subthreshold states of ^{16}O and compared them with the existing values in the literature. The ANC value for the 6.92 MeV (2^+) state from this work agrees with most of the earlier works within error bars. Using the present ANC values, R -matrix calculations for the g.s. $E1$ and $E2$ S -factors of the $^{12}\text{C}(\alpha,\gamma)^{16}\text{O}$ reaction were carried out and compared with existing data. The impact of the g.s. ANC is also studied. The present work depicts an independent channel to study the important $^{12}\text{C}(\alpha,\gamma)^{16}\text{O}$ radiative capture reaction in nuclear astrophysics. The subthreshold doublets could not be separated,

and further measurements would be useful for a better extraction of the ANC.

Data availability

Data will be made available on request.

Declaration of competing interest

The authors declare that they have no known competing financial interests or personal relationships that could have appeared to influence the work reported in this paper.

Acknowledgements

The authors thank the ISOLDE engineers in charge, RILIS team and Target Group at CERN for their support. D. Gupta acknowledges research funding from the European Union's Horizon 2020 research and innovation programme under grant agreement no. 654002 (ENSAR2) and ISRO, Government of India under grant no. ISRO/RES/2/378/15-16. R. Mitra acknowledges the support of DST-INSPIRE fellowship (DST/INSPIRE/03/2021/000155, IF No. IF200499). O. Tengblad would like to acknowledge the support by the Spanish Funding Agency (AEI / FEDER, EU) under the project PID2022-140162NB-I00. I. Martel would like to acknowledge partial support by Grant PID2021-127711NB-I00 (2021) of the Spanish Government. J. Cederkall acknowledges the Swedish Research Council under the grants 2021-00174-VR, 2021-04575-VR, 2017-00637-VR and 2017-03986-VR. A.M.M. is supported by the grants PID2020-114687GB-I00 and PID2023-146401NB-I00 by MICIU/AEI/10.13039/501100011033.

References

- [1] R.J. Jaszczak, et al. Phys. Rev. C 2 (1970) 63–2452.
- [2] W.A. Fowler, Les Prix Nobel Almquist. Wiksell Int, Stockholm, Sweden, 1983.
- [3] K. Langanke, C.A. Barnes, Adv. Nucl. Phys. 22 (2025) 173–263.
- [4] T.A. Weaver, S.E. Woosley, Phys. Rep. 227 (1993) 65.
- [5] G. Wallerstein, Rev. Mod. Phys. 69 (1997) 995.
- [6] R.J. Deboer, Rev. Mod. Phys. 89 (2017) 35007.
- [7] N. Oulebsir, Phys. Rev. C 85 (2012) 35804.
- [8] <http://www.astro.ulb.ac.be/nacree/>.
- [9] S.E. Woosley, Rev. Mod. Phys. 74 (2002) 1015.
- [10] A. Redder, Nucl. Phys. A 462 (1987) 385.
- [11] A. Belhout, et al., Nucl. Phys. A 793 (2007) 178. See references therein.
- [12] R. Smith, Nat. Commun. 12 (2021) 5920.
- [13] S. Adhikari, Phys. Rev. C 89 (2014) 44618.
- [14] Y.P. Shen, Prog. Part. Nucl. Phys. 119 (2021) 103857. See references therein.
- [15] Y.P. Shen, Phys. Rev. C 99 (2019) 25805.
- [16] F.D. Becchetti, Nucl. Phys. A 305 (1978) 293.
- [17] F.D. Becchetti, Nucl. Phys. A 305 (1978) 313.
- [18] N. Keeley, Phys. Rev. C 66 (2002) 44605.
- [19] A.T. Rudchik, Eur. Phys. J. A 41 (2009) 31–37.
- [20] Sgouros, Phys. Rev. C 94 (2016) 44623.
- [21] M. Mazzocco, Phys. Rev. C 92 (2015) 24615.
- [22] H. Amro, Eur. Phys. J. Spec. Top. 150 (2007) 1–4.
- [23] F.D. Becchetti, Phys. Rev. Lett. 34 (1975) 225.
- [24] M.E. Cobern, Phys. Rev. C 14 (1976) 491.
- [25] Kolata, Eur. Phys. J. A 52 (2016) 123.
- [26] K. Kundalia, Phys. Lett. B 833 (2022) 137294.
- [27] R. Plag, Phys. Rev. C 86 (2012) 15805.
- [28] A.J. Selove, Nucl. Phys. A 490 (1988) 1–225.
- [29] W.D. Weintraub, Phys. Rev. C 100 (2019) 24604.
- [30] I.J. Thomson, Comput. Phys. Rep. 7 (1988) 167.
- [31] R.W. Zurmühle, C.M. Fou, Nucl. Phys. A 129 (1969) 502.
- [32] C.M. Perey, F.G. Perey, At. Data Nucl. Data Tables 17 (1976) 1.
- [33] B. Buck, J. Phys. G 14 (1988).
- [34] C.A. Bertulani, Phys. Rev. C 49 (1994) 2688.
- [35] M. Vorabbi, Phys. Rev. C 100 (2019) 24304.
- [36] V. Burjan, Front. Astron. Space Sci. 7 (2020) 562466.
- [37] K. Wildermuth, Y.C. Tang, A Unified Theory of the Nucleus, New York, Academic Press, 1977.
- [38] Y. Suzuki, Prog. Theor. Phys., volume 55 (6) (1976) 1751–1768.
- [39] J. Dobaczewski, J. Phys. G 41 (2014) 74001.
- [40] S. Adhikari, J. Phys. G 44 (2017) 15102.
- [41] M.C. Morais, R. Lichtenthäler, Nucl. Phys. A 857 (2011) 1.
- [42] S. Adhikari, Phys. Lett. B 682 (2009) 216.

- [43] Y.P. Shen, Phys. Rev. Lett. 124 (2020) 162701.
- [44] A.K. Mondal, Int. J. Mod. Phys. 30 (2021) 2150039.
- [45] C.R. Brune, Phys. Rev. Lett. 83 (1999) 4025.
- [46] S. Adhikari, Phys. Lett. B 704 (2011) 308–311.
- [47] M.L. Avila, Phys. Rev. Lett. 114 (2015) 71101.
- [48] A. Mondal, et al. Phys. Lett. B 772 (2017) 216.
- [49] R.E. Azuma, Phys. Rev. C 81 (2010) 45805.
- [50] E. Uberseder, R.J. Deboer, AZURE2 User Manual, 2015.
- [51] J.W. Hammer, Nucl. Phys. A 752 (2005) 514.
- [52] J.W. Hammer, Nucl. Phys. A 758 (2005) 363.